# On the Kantorovich approach for calculations of the hydrogen atom states affected by a train of short pulses

O. Chuluunbaatar[a], A.A. Gusev[a], V.L. Derbov[b], M.S. Kaschiev[c], K.A. Kouzakov[d], V.V. Serov[b], V.N. Samoylov[a], T.V. Tupikova[a], S.I. Vinitsky[a]

[a] Joint Institute for Nuclear Research, Dubna, Moscow Region, Russia
[b] Saratov State University, Russia
[c] Institute of Mathematics and Informatics, BAS, Sofia, Bulgaria
[d] Research Institute for Nuclear Physics, Moscow State University, Russia

## ABSTRACT

We present theoretical calculations for the evolution of Zeeman states in a train of short electric half-cycle pulses (kicks). For the numerical solution of the corresponding time-dependent Schrödinger equation (TDSE) the high-accuracy splitting scheme based on the unitary approximations of the evolution operator is developed. The finite element method is used for determining the spatial form of the solution. The efficiency and stability of the developed computational method is shown for 1D models in the cases of second-, forth-, and sixth-order accuracy with respect to the time step. Numerical calculations for the kicked hydrogen atom in the presence of magnetic field are performed using the scheme of the sixth-order accuracy with respect to a time step and both Galerkin and Kantorovich reductions of the problem with respect to the angular variables. For a particular choice of the electric- and magnetic-field parameters and the initial Zeeman state the corresponding results exhibit a two-state resonance picture.

**Keywords:** time-evolution operator, half-cycle pulses, high-order operator-difference schemes, kicked hydrogen atom, magnetic field, Galerkin and Kantorovich methods

## 1. INTRODUCTION

The dynamics of a charged particle in a combined constant magnetic and time-dependent electric field exhibits a number of remarkable phenomena. For example, the classical electron trajectory calculations show that the electromagnetic radiation of the relativistic electron in a constant magnetic field and an ultrashort intense laser pulse possesses a rich structure in both magnetic and electric field directions.[1] If a resonance condition between the cyclotron frequency and the laser frequency is met the radiation losses are minimized and an extreme electron acceleration becomes possible within a very short travel distance of the electron.[2] A solution of Dirac equation for atomic electron in a combined strong magnetic and laser field yields a ring-shaped electron distribution in the resonance regime.[3] Application of static magnetic field may enhance the ionization rate or stabilize a quantum system in intense laser pulse.[4] The same effect is observed for a model zero-range potential system.[5] Moreover, not only the one-electron dynamics but the many-electron dynamics as well can be nontrivially controlled using the crossed magnetic and electric field configuration.[6] These findings indicate a rich potential for controlling the dynamics of classical and quantum systems by employing a combination of magnetic and electric fields with various parameters.

In the quantum case, for solving the control problem one should resort to the solution of time-dependent Schrödinger equation (TDSE). It should be stressed that an accurate solution of the TDSE is of prime importance for a wide range of quantum mechanical applications. In particular, the theory of phenomena induced by short electric-field pulses in atoms and ions often relies on the numerical treatments of the evolution problem. The results of these numerical calculations are crucial for predictions of various effects, for example, such as the dynamical stabilization of an atom in intense laser radiation.[7,8] Needless to say that here the stability and

Further author information: Send correspondence to Sergue Vinitsky, E-mail: vinitsky@thsun1.jinr.ru

Saratov Fall Meeting 2005: Laser Physics and Photonics, Spectroscopy and Molecular Modeling VI, edited by Vladimir L. Derbov, Leonid A. Melnikov, Lev M. Babkov, Proc. of SPIE Vol. 6165, 61650C, (2006) · 0277-786X/06/$15 · doi: 10.1117/12.696846

accuracy of utilized numerical scheme become a key factor in determining (or not) the above-mentioned effect. In addition, the employed numerical algorithm should be efficient for the implementation on nowadays computers.

The modern laser physics experiments have stimulated computer simulations of the dynamics of Coulomb systems (including exotic ones) in a train of laser pulses.[9–13] In this case a necessity of constructing the unitary splitting algorithms[14] has emerged.[13,15] There are two major requirements for the numerical methods that are being developed. Namely, they must be stable and must provide a high accuracy in both time and space. In this respect the unitary splitting methods have a very important advantage: the unitarity of the evolution operator preserves the norm of the wave function and thus guarantees a conservation of the probability and a stability of the method. Since the unitary splitting methods involve a finite time grid, the other part of the computational problem consists in determining for each time step an accurate form of the solution in space. It can be solved using the space-discretization techniques, where instead of approximating the wave packet by a globally defined basis one involves suitable interpolation polynomials on a finite space grid. The required accuracy of the solution with respect to the spatial step can be achieved using the finite element method (FEM).[16,17] User-friendly symbolic algorithms implemented with the help of MAPLE and REDUCE allow one to generate stable implicit operator–difference and multilayer grid schemes, as well as the corresponding FORTRAN codes for the numerical solution of the evolution problem for the TDSE on a finite interval with prescribed accuracy both in time and space variables.[18] The corresponding effective Hamiltonians and algebraic matrix problems are generated on the basis of the methods of splitting for the unitary evolution operator on a time-uniform grid and the finite-element method for the space variable. An important element of the algorithm proposed is the auxiliary gauge transformation, which allows one to obtain, for real Hamiltonians, the algebraic problems with complex symmetrical matrices on local carriers. This ensures the efficiency of the employment of the finite-element method.[19]

In this work we formulate a computational method for solving TDSE which is based on the unitary splitting algorithm involving a uniform time grid.[20–22] For numerical implementation of this method we derive the second-, forth-, and sixth-order approximations with respect to the time step. Both Galerkin and Kantorovich reductions of the problem, as well as FEM are used to construct the numerical schemes of required accuracy with respect to the spatial step.[23–25] We establish the efficiency and accuracy of the developed numerical scheme considering the case of a kicked hydrogen atom in the absence of magnetic field. The case of Zeeman states kicked by a train of short electric half-cycle pulses is then treated within the present computational method. The numerical calculations are performed for various initial states using the physically realistic values of electric and magnetic field parameters.

The paper is organized as follows. In Section 2 we formulate the method of solving TDSE that consists in the construction and decomposition of the Time-Evolution Operator and further generation of unitary operator-difference schemes with partial splitting of the evolution operator of high order with respect to the time step. In Section 3 the applications of the elaborated schemes till the sixth order with respect to time step are shown using the conventional 1D models, namely, the oscillator in an external periodical field, approximated by a train of $\delta$ kicks, and the Pöschl-Teller atom in a laser pulse field. In Section 4 we present realization of the schemes with both Galerkin and Kantorovich reduction for kicked 3D hydrogen atom in a magnetic field. Some results of the corresponding numerical experiments are shown in Section 5. In Section 6 the conclusions are made and the possible future applications of the method are discussed.

## 2. FORMULATION OF THE METHOD

The TDSE governing the dynamics of an atom in an external field in the time interval $t \in [t_0, t_{max}]$ reads:

$$i\frac{\partial\psi(\vec{r},t)}{\partial t} = H(\vec{r},t)\psi(\vec{r},t), \qquad \psi(\vec{r},t_0) = \psi_0(\vec{r}), \quad \psi(\vec{r},t) \in \mathrm{H}^1(\mathrm{R}^n \otimes [t_0,t_{max}]), \qquad \psi_0(\vec{r}) \in \mathrm{H}^1(\mathrm{R}^n). \quad (1)$$

We assume the Hamiltonian to obey the form

$$H(\vec{r},t) = H_0(\vec{r}) + Q(\vec{r},t), \qquad H_0(\vec{r}) = -\frac{1}{2}\Delta_{\vec{r}} + V(\vec{r}), \quad (2)$$

where $V(\vec{r})$ is the static continuous potential function, and the potential function $Q(\vec{r},t)$ describes the interaction of an atom with a time-dependent external field. The normalization condition is

$$||\psi||^2 = \int |\psi(\vec{r},t)|^2 d\vec{r} = 1, \qquad t \in [t_0, t_{max}]. \tag{3}$$

Consider now the initial problem on a uniform time grid $\Omega_\tau = \{t_0,\ t_{k+1} = t_k + \tau\ (k = 0,1,\ldots,K-1),\ t_K = t_{max}\}$. The solution $\psi(t_{k+1}) \equiv \psi(\vec{r},t_{k+1})$ is derived from the solution $\psi(t_k)$ by means of the unitary evolution operator $U$:

$$\psi(t_{k+1}) = U(t_{k+1},t_k)\psi(t_k).$$

The operator $U(t_{k+1},t_k)$ can be presented in the form:

$$U(t_{k+1},t_k) \equiv U(t_{k+1},t_k;\tau) = \exp(-i\tau A_k),$$

where $A_k$ is the effective time-independent Hamiltonian related to $H(t)$ through the Magnus expansion:

$$A_k = \frac{1}{\tau}\int_{t_k}^{t_{k+1}} dt H(t) + \frac{i}{2\tau}\int_{t_k}^{t_{k+1}} dt' \int_{t_k}^{t'} dt''[H(t''),H(t')] + \cdots. \tag{4}$$

Using the Taylor-series expansion of $H(t)$ in the vicinity of $t = t_k + \tau/2$ and performing the integrations, one can derive a set of the operators $A_k^{(M)}$ $(M = 1,2,\ldots)$ such that

$$\begin{aligned}
&A_k = A_k^{(M)} + O(\tau^{2M}), \quad A_k^{(M)} = \hat{A}_k^{(M)} + \imath\breve{A}_k^{(M)}, \\
&\hat{A}_k^{(1)} = H, \qquad \breve{A}_k^{(1)} = 0, \\
&\hat{A}_k^{(2)} = \hat{A}_k^{(1)} + \frac{\tau^2}{24}\ddot{H}, \qquad \breve{A}_k^{(2)} = \breve{A}_k^{(1)} + \frac{\tau^2}{12}(adH)\,\dot{H}, \\
&\hat{A}_k^{(3)} = \hat{A}_k^{(2)} + \frac{\tau^4}{1920}\ddddot{H} - \frac{\tau^4}{720}(adH)^2\,\ddot{H} - \frac{\tau^4}{240}(ad\,\dot{H})^2 H, \\
&\breve{A}_k^{(3)} = \breve{A}_k^{(2)} - \frac{\tau^4}{480}(ad\,\dddot{H})H + \frac{\tau^4}{480}(ad\,\ddot{H})\,\dot{H} + \frac{\tau^4}{720}(adH)^3\,\dot{H},
\end{aligned} \tag{5}$$

where the dot over $H \equiv H(t)$ means the derivative with respect to $t$ at $t = t_k + \tau/2$. Thus, we have the following approximate expression of the evolution operator

$$U(t_{k+1},t_k;\tau) = \exp(-i\tau A_k^{(M)}) + O(\tau^{2M+1}).$$

## 2.1. Operator-difference scheme

The exponential operator can be presented in the form of the generalized $[M/M]$ Padé approximation with the same accuracy

$$\exp(-i\tau A_k^{(M)}) = \prod_{\zeta=1}^{M} T_{\zeta k} + O(\tau^{2M+1}), \quad T_{\zeta k} = \frac{I + (\tau/2M)\alpha_\zeta^{(M)} A_k^{(M)}}{I + (\tau/2M)\bar{\alpha}_\zeta^{(M)} A_k^{(M)}},$$

where the coefficients $\alpha_\zeta^{(M)}$ $(\zeta = 1,\ldots,M)$ are the roots of the equation ${}_1F_1(-M,-2M,2Mi/\alpha) = 0$ with ${}_1F_1$ being a confluent hypergeometric function, and $\bar{\alpha}_\zeta^{(M)}$ is the complex conjugate of $\alpha_\zeta^{(M)}$. The coefficients $\alpha_\zeta^{(M)}$ have the following properties: $\mathrm{Im}(\alpha_\zeta^{(M)}) < 0$ and $0.6 < |\alpha_\zeta^{(M)}| < \mu^{-1}$, where $\mu$ is a root of the equation $\mu\exp(\mu+1) = 1$ $(\mu \approx 0.28)$. Note that the condition

$$0 < \tau_0 \le \tau < 2M\mu||A_k^{(M)}||^{-1} \tag{6}$$

**Table 1.** Real and imaginary parts of coefficients $\alpha_\zeta^{(M)}$, $M = 1, 2, 3$, $\zeta = 1, ..., M$

| M | $\zeta$ | $\Re\alpha_\zeta$ | $\Im\alpha_\zeta$ |
|---|---|---|---|
| 1 | 1 | +0.00000000000000000000000000000 | −1.00000000000000000000000000000 |
| 2 | 1 | −0.57735026918962576450914878050 | −1.00000000000000000000000000000 |
| 2 | 2 | +0.57735026918962576450914878050 | −1.00000000000000000000000000000 |
| 3 | 1 | −0.81479955424892281841473623156 | −0.85405673065166346526579940886 |
| 3 | 2 | +0.00000000000000000000000000000 | −1.29188653869667306946840118228 |
| 3 | 3 | +0.81479955424892281841473623156 | −0.85405673065166346526579940886 |

guarantees the validity of the approximation for any bounded operator $A_k^{(M)}$.

Using the approximate form for the evolution operator, it is convenient to introduce the following auxiliary functions:

$$\psi_{k+\zeta/M} = T_{\zeta k}\psi_{k+(\zeta-1)/M}, \qquad \zeta = 1, \ldots, M. \tag{7}$$

Since $\mathrm{Im}(\alpha_\zeta^{(M)}) < 0$, the operators $T_{\zeta k}$ are isometric and, therefore,

$$\|\psi_k\| = \|\psi_{k+1/M}\| = \ldots = \|\psi_{k+1}\|. \tag{8}$$

The auxiliary functions $\psi_{k+\zeta/M}$ $(\zeta = 1, ..., M)$ can be treated as approximate solutions at the mesh points $t_{k+\zeta/M} = t_k + \tau\zeta/M$ $(\zeta = 1, ..., M)$ in the time interval $[t_k, t_{k+1}]$.

Using the above approximation for each time step of the grid $\Omega_\tau$, the following operator-difference scheme for the numerical solution of the Schrödinger equation can be formulated:

$$\begin{aligned} \psi_0 &= \psi(t_0), \\ \left(I + \frac{\tau}{2M}\bar{\alpha}_\zeta^{(M)} A_k^{(M)}\right)\psi_{k+\zeta/M} &= \left(I + \frac{\tau}{2M}\alpha_\zeta^{(M)} A_k^{(M)}\right)\psi_{k+(\zeta-1)/M}, \\ \psi(t_{max}) &= \psi_K \qquad (\zeta = 1, \ldots, M,\ k = 0, 1, \ldots, K-1). \end{aligned} \tag{9}$$

This is an implicit numerical scheme of the order $2M$. It is stable because it conserves the norm of the difference solution. Note, that in the case $M = 1$ we have $\alpha_1^{(1)} = -i$ and this scheme is reduced to the well-known Crank-Nicholson algorithm (see also Table 1).

## 2.2. Unitary schemes with partial splitting of the evolution operator

To illuminate the imaginary part $\breve{A}_k^{(M)}$ of the effective operators $A_k^{(M)} = \hat{A}_k^{(M)} + \imath\breve{A}_k^{(M)}$ from (5) in Eqs. (9) we will use a gauge transformation

$$\tilde{\psi} = \exp\left(\imath S_k^{(M)}\right)\psi,$$

that yields the new effective operators

$$\tilde{A}_k^{(M)} = \exp\left(\imath S_k^{(M)}\right) A_k^{(M)} \exp\left(-\imath S_k^{(M)}\right).$$

Here $S_k^{(M)}$ is found in the form $S_k^{(M)} = \sum_{j=0}^{2M} \tau^j S_j$ with unknown coefficients $S_j$, derived from the relations[19]

$$\breve{\tilde{A}}_k^{(M)}\ \hat{\psi} = O(\tau^{2M}), \qquad \breve{\tilde{A}}_k^{(M)} = \exp\left(\imath S_k^{(M)}\right)\breve{A}_k^{(M)} \exp\left(-\imath S_k^{(M)}\right).$$

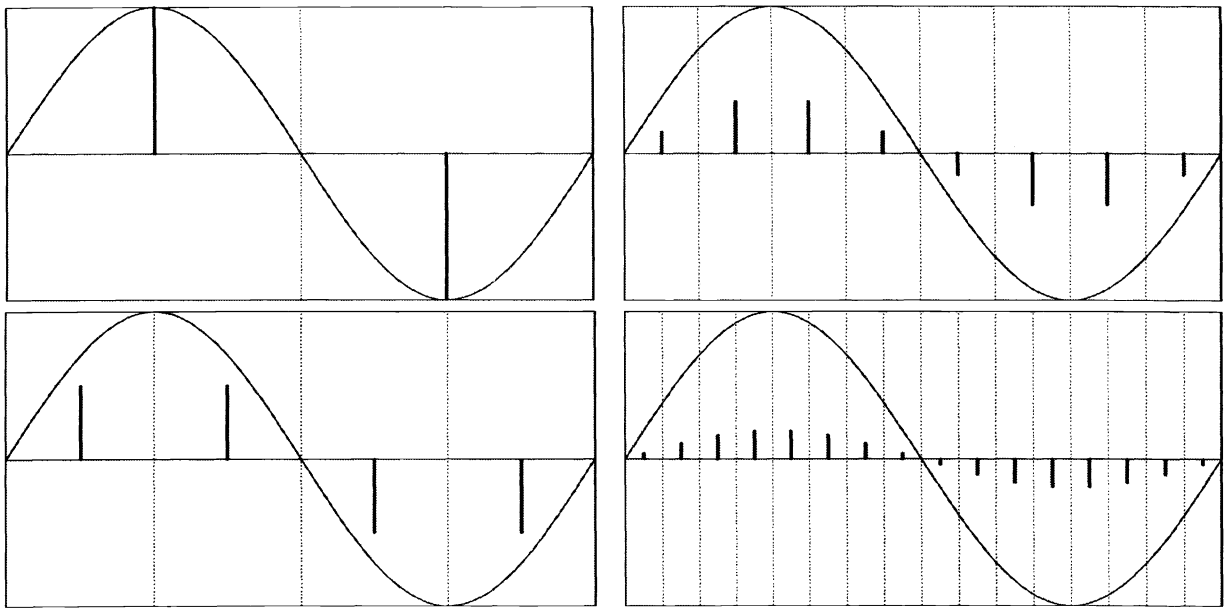

**Figure 1.** Approximations of the external field $f(t) = f_0 \sin(\omega_0 t)$ by 2, 4, 8, 16 kicks

In this case in each $k$- time step of the grid $\Omega_\tau$ for an approximate solution of the TDSE we have the following operator-difference scheme:

$$\begin{aligned} \tilde{\psi}^0 &= \exp\left(\imath S_k^{(M)}\right)\psi(t_k), \\ \left(I + \frac{\tau}{2M}\overline{\alpha}_\zeta^{(M)}\tilde{A}_k^{(M)}\right)\tilde{\psi}^{\zeta/M} &= \left(I + \frac{\tau}{2M}\alpha_\zeta^{(M)}\tilde{A}_k^{(M)}\right)\tilde{\psi}^{(\zeta-1)/M}, \\ \psi(t_{k+1}) &= \exp\left(-\imath S_k^{(M)}\right)\tilde{\psi}^1 \qquad (\zeta = 1,\ldots,M,\ k = 0,1,\ldots,K-1). \end{aligned} \tag{10}$$

to make the FEM good use. Note, that if $S_{t_c}^{(M)}$ is not a multiplication operator, then the exponential operators in (10) can be decomposed as well.[18]

## 3. EXAMPLE: 1D MODEL ATOM IN AN EXTERNAL FIELD.

For the Hamiltonian of 1D model atom under the action of the external field $f(t)$ in the dipole approximation

$$H(x,t) = -\frac{1}{2}\frac{\partial^2}{\partial x^2} + V(x) + xf(t), \tag{11}$$

at each $k$-th step of the scheme (10) we have the operators $\tilde{A}_k^{(M)}$ and $S_k^{(M)}$ for $M = 1,2,3$ in the form

$$\begin{aligned} \tilde{A}_k^{(1)} &= H(x,t_c), & S_k^{(1)} &= 0, \\ \tilde{A}_k^{(2)} &= \tilde{A}_k^{(1)} + x\frac{\partial^2 f(t_c)}{\partial t^2}, & S_k^{(2)} &= S_k^{(1)} + \frac{\tau^2}{12}x\frac{\partial f(t_c)}{\partial t}, \\ \tilde{A}_k^{(3)} &= \tilde{A}_k^{(2)} + \frac{\tau^4}{1920}x\frac{\partial^4 f(t_c)}{\partial t^4} + \frac{\tau^4}{1440}f(t_c)\frac{\partial^2 f(t_c)}{\partial t^2} + \frac{\tau^4}{1440}\left(\frac{\partial f(t_c)}{\partial t}\right)^2 + \frac{\tau^4}{720}\frac{\partial V(x)}{\partial x}\frac{\partial^2 f(t_c)}{\partial t^2}, \\ S_k^{(3)} &= S_k^{(2)} - \frac{\tau^4}{720}\frac{\partial V(x)}{\partial x}\frac{\partial f(t_c)}{\partial t} + \frac{\tau^4}{480}x\frac{\partial^3 f(t_c)}{\partial t^3}. \end{aligned}$$

Note, that in further analysis we will use the FEM. Then the new operators in both sides of Eqs. (10) can appear presented by the symmetric complex band matrices[18,19] for which subroutines of the FEM[17] can be used

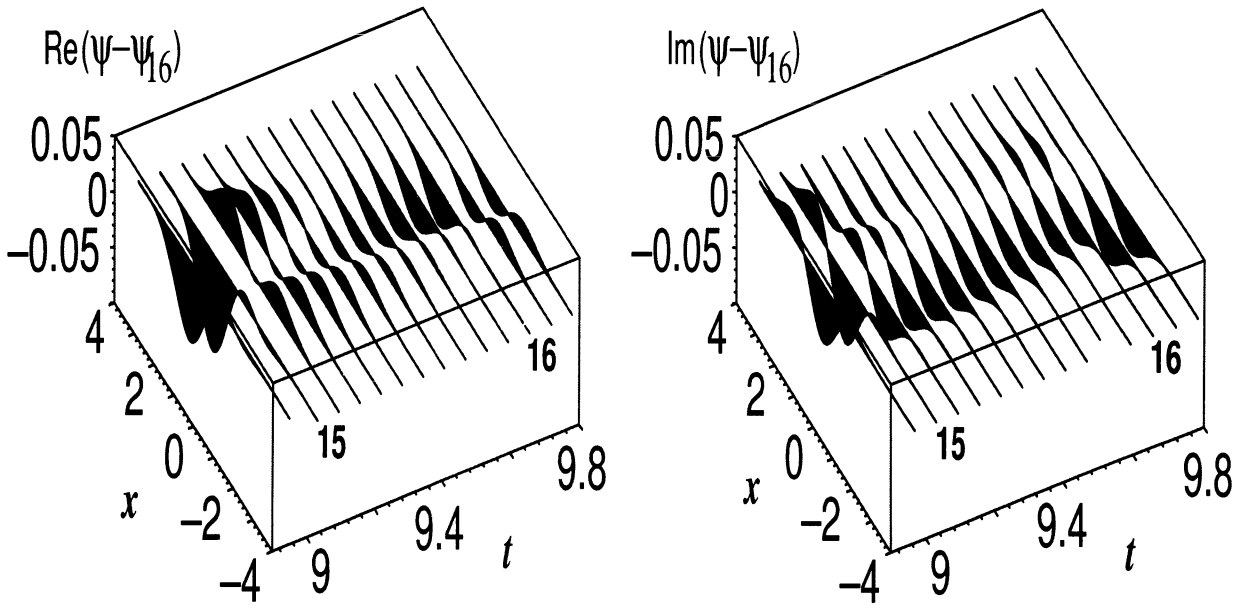


**Figure 2.** Real and imaginary parts of the difference between the analytical solutions for the oscillator in the continuous field (12) and for the discrete approximation (13) of this continuous field by 16 kicks. The time moments of 15 and 16 kicks $t_{15} = 9.0625$, $t_{16} = 9.6875$ are indicated by the corresponding numbers.

to reduce the necessary computational resources. Generally, the old operators in both sides of Eqs. (9) can be presented by nonsymmetric complex band matrices for $M \geq 2$.

### 3.1. Exact solvable model: Oscillator in an external periodical field.

Now we consider the above problem (11) with the potential function

$$V(x) = \omega^2 x^2/2$$

that supports only a pure discrete spectrum. This potential describes a harmonic oscillator with the angular frequency $\omega$. Let the external field be harmonic

$$f(t) = f_0 \sin(\omega_0 t) \tag{12}$$

with the strength $f_0$ and the angular frequency $\omega_0$. Let approximate the external field by a set of $\delta$ functions in a uniform grid[27] (see also Fig. 1):

$$f_d(t) = \sum_{s=1}^{S} \delta(t - T(s-1/2)) \int_{T(s-1)}^{Ts} f(t)dt, \tag{13}$$

where $T = 2\pi/\omega_0/N$ is the interval between kicks at fixed integer $N \geq 1$ and $S$ is the number of kicks. We choose the initial state $\psi_0(x)$ at the time $t_0 = 0$ as a Gaussian wave packet

$$\psi_0(x) = \sqrt[4]{\omega/\pi} \exp(-\omega(x - x_0)^2/2 + \imath p_0(x - x_0)).$$

For the numerical example considered below the constants are taken to be $x_0 = 0$, $p_0 = 0$, $\omega = 1$, $\omega_0 = \pi/5$, $f = 0.5$. This problem is a very good test for numerical experiments because it has the known analytical solutions $\psi(x,t)$ in both continuous (12) and discrete (13) cases that are generated explicitly using MAPLE. As an example, the differences between these solutions are shown in Fig. 2.

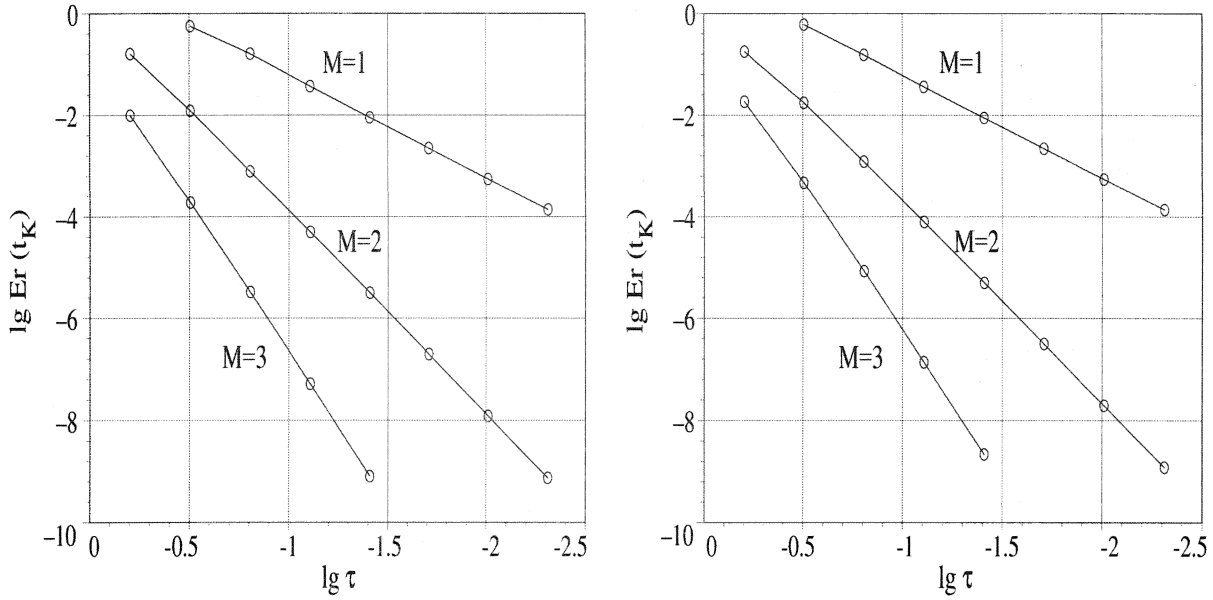


**Figure 3.** Logarithm of discrepancy $\lg_{10} Er(t_K)$ for the schemes with $M = 1, 2, 3$ as a function of the time step $\tau$ at $t_K = 10$, calculated for the oscillator in the continuous field (left panel) and in the field approximated by 4 kicks (right panel), $t \in [0, 10]$.

In the numerical experiments we consider the finite element grid $\Omega_h^p$ with 1000 elements of the order $p = 6$ in the interval $[x_{min}, x_{max}]$, where $x_{min} = 20$, $x_{max} = 20$, and $0 \le t \le 10$. We use the enclosed three time grids $\Omega_\tau[0, 10]$ with the step $\tau$ taking the values $\tau = 0.005, 0.0025, 0.00125$ and examine the behavior of the function

$$Er^2(t; i) = \int_{x_{min}}^{x_{max}} [\psi(x,t) - \psi_i(x,t)]^* [\psi(x,t) - \psi_i(x,t)] dx, \tag{14}$$

where the index $i = 1, 2, 3$ labels the numerical solutions, obtained for different values of the time step $\tau$. Having these three values of $Er(t; i)$, we can calculate the Runge ratio

$$\alpha_M(t) = \ln \frac{|Er(t;1) - Er(t,2)|}{|Er(t;2) - Er(t,3)|} / \ln 2. \tag{15}$$

Hence, we obtain the following theoretical estimates: $\alpha_1(t) \approx 2$ for the scheme with $M = 1$, $\alpha_2(t) \approx 4$ for the scheme with $M = 2$ and $\alpha_3(t) \approx 6$ for the scheme with $M = 3$. In Fig. 3 one can see the declared rate of convergence $O(\tau^{2M})$ with respect to $\tau$.

### 3.2. The Pöschl-Teller atom in a laser pulse field.

Now we consider the propagation problem (11) for the PT model with the potential function $V(x) = -\cosh^{-2} x$ that supports only one bound state

$$\psi_0(x) = 1/(\sqrt{2}\cosh x),$$

with the eigenvalue $E_0 = -0.5$ a.u., and a continuum of scattering states

$$\psi^{(+)}_{1,2E}(x) = \frac{1}{\sqrt{2\pi}} \frac{\imath|k| \mp \tanh x}{1 + \imath|k|} \exp(\imath k x)$$

with $E = k^2/2$, 1 corresponding to $k > 0$, 2 corresponding to $k < 0$.[28,29] The laser pulse $f(t)$ is given by

$$f(t) = \left\{ f_0 \sin^2\left(\frac{\pi t}{2t_p}\right), 0 < t < 2t_p; 0, t \ge 2t_p, \right\},$$

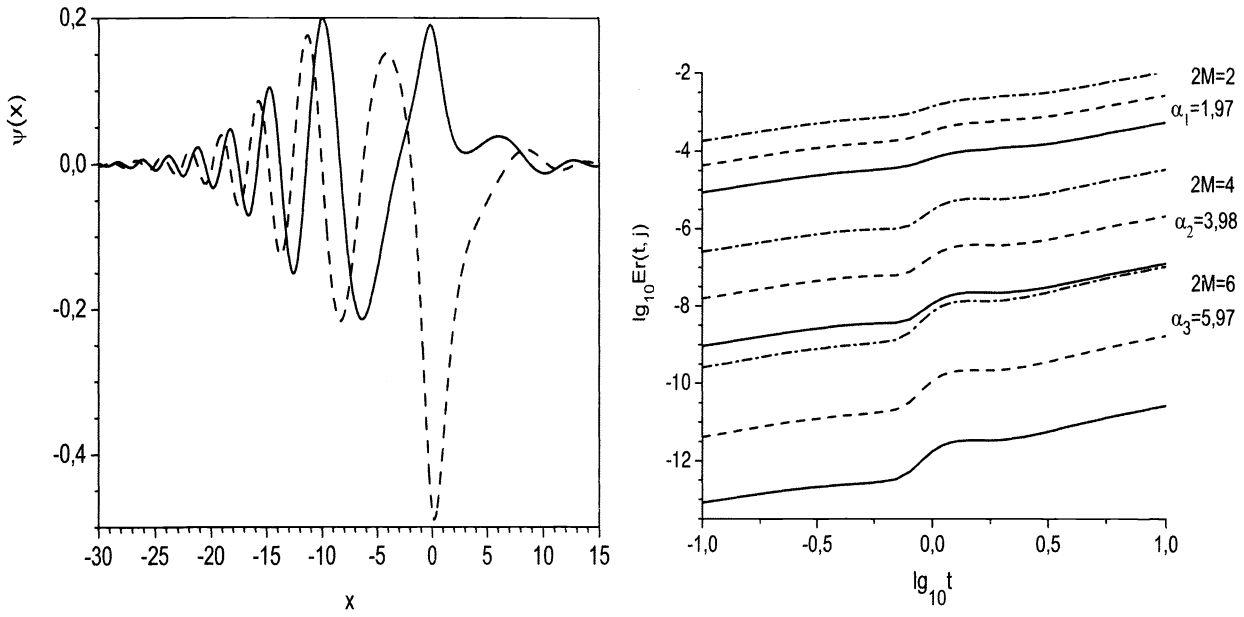


**Figure 4.** Real (solid) and imaginary (dashed) parts of the solution $\phi(x,t)$ for PTA atom at $t = T = 10$ (left panel) and logarithm of discrepancy $Er(t;i), i = 1,2,3$ (dash-dotted, dashed and solid curves for schemes with $M = 1,2,3$, respectively) calculated using Fortran with quadruple precision (33 significant digits) (right panel).

where $f_0 = t_p = 1$.

To approximate the solution $\psi_i(x,t)$, $i = 1,2,3,4$ we use 1600 finite elements with $p = 6$ and the finite element grid

$$\Omega = \{-1500(200) - 300(200) - 20(200) - 1(400)1(200)20(200)300(200)1500\},$$

where the numbers in brackets denote the number of finite elements in the intervals.

We calculated the above solution over the enclosed time grids $\Omega_\tau[t_0 = 0, T = 10]$ with four different time steps $\tau = 0.01, 0.005, 0.0025, 0.00125$. Fig. 4 displays the wave function calculated at $T = 10$ and the behavior of the discrepancies $Er(t;i), i = 1,2,3$ evaluated using Eqs. (14) at $M = 1,2,3$. The Runge ratio was calculated using Eq. (15) where the function $\psi_4(x,t)$ was used instead of the analytical solution $\psi(x,t)$. The numerical estimations of $\alpha_M(t)$ and its mean value, $\alpha_M \approx 2M$ are close to the theoretical ones.

## 4. THE KICKED HYDROGEN ATOM

$\delta$-kicks provide a widely used approximation of electric-field pulses that are much shorter than the classical orbital period of the atom. The Hamiltonian of a kicked hydrogen atom in the presence of the constant magnetic field parallel to the $z$ axis is given by

$$H = H_0 + V_{ext}, \qquad H_0 = -\frac{1}{2}\Delta_{\vec{r}} - \frac{1}{r} + V_Z, \qquad V_{ext} = -\sum_{s=1}^{S}(\vec{r}\vec{F}_s)\delta(t - sT), \tag{16}$$

where $S$ is the total number of kicks, $T$ is the period of kicks, and $\vec{F}_s$ is the amplitude of the $s$th kick. The term $V_Z$ accounts for the interaction of the atom with the magnetic field

$$V_Z(r) = \frac{\imath\beta}{2}\frac{\partial}{\partial\varphi} + \frac{1}{8}\beta^2 r^2[\beta_z + (1 - \beta_z)\sin^2\theta], \tag{17}$$

where $\beta$ is the strength of the magnetic field and $\beta_z$ is the quadruple deformation parameter.

We consider the model of unidirectional kicks (half-cycle pulses) and assume that the electric field coincides with the $z$ axis, so that $(\vec{r}\vec{F}_s) = zF_s$. Therefore, the $z$ component of the orbital angular momentum is conserved and $m$ is a magnetic quantum number. Furthermore, it is convenient to work with parabolic states. If the magnetic field is absent ($\beta = 0$), we utilize the following formulas for the orthogonal transformation relating the parabolic states to the usual hydrogen atom states:

$$\Phi^{(0)}_{n_1 n_2 m}(\vec{r}) = \sum_{l=|m|}^{n-1} A^{n_1 n_2}_{nlm} \Phi^{(0)}_{nlm}(\vec{r}), \quad \Phi^{(0)}_{nlm}(\vec{r}) = \sum_{n_1,n_2=0}^{n-|m|} A^{n_1 n_2}_{nlm} \Phi^{(0)}_{n_1 n_2 m}(\vec{r}). \tag{18}$$

Here $n = n_1 + n_2 + |m| + 1$ is the principal quantum number, and the matrix elements $A^{n_1 n_2}_{nlm}$ are known. In the presence of the magnetic field the initial state $\psi_0(\vec{r})$ is an eigenfunction of the Hamiltonian $H_0$. In the case of weak magnetic fields this state can also be specified by the principal quantum number $n$.

### 4.1. Free evolution

In the interval between the $(s-1)$th and $s$th kicks the atom evolves freely according to the TDSE

$$i\,\frac{\partial\psi(\vec{r},t)}{\partial t} = H_0\psi(\vec{r},t), \qquad \psi(\vec{r},t) \in H^1\left(R^3 \otimes ((s-1)T_+, sT_-)\right), \tag{19}$$

where $T_\pm = T \pm 0$. The formal solution for the wave function $\psi(t) \equiv \psi(\vec{r},t)$ is given by

$$\psi(t+\delta t) = \exp(-i\,H_0\delta t)\psi(t). \tag{20}$$

Using the above scheme in the time interval $((s-1)T_+, sT_-)$, we obtain a set of equations

$$\begin{aligned} \hat{\psi}_0 &= \psi((s-1)T_+), \\ \left(I + \frac{\bar{\alpha}^{(M)}_\zeta H_0\tau}{2M}\right)\hat{\psi}_{k+\zeta/M} &= \left(I + \frac{\alpha^{(M)}_\zeta H_0\tau}{2M}\right)\hat{\psi}_{k+(\zeta-1)/M}, \\ \psi(sT_-) &= \hat{\psi}_K \qquad (\zeta = 1,\ldots,M \text{ and } k = 1,\ldots,K-1). \end{aligned}$$

### 4.2. Single kick

To illustrate the computational algorithm for periodic $\delta$-kicks, we consider the Schrödinger equation for a single kick at the moment $t = sT$:

$$i\,\frac{\partial\psi(\vec{r},t)}{\partial t} = [H_0 - zF_s\delta(t-sT)]\psi(\vec{r},t), \qquad \psi(\vec{r},t) \in H^1(R^3 \otimes (sT_-, sT_+)). \tag{21}$$

The case of several kicks is then treated by repeating the computational steps outlined below for a single kick. Thus, the same method also allows one to handle the cases of non-periodic and non-equal kicks as well as of alternating kicks. We employ the following formula for calculating the wave function $\psi(\vec{r}, sT_+)$ immediately after the kick ($t = sT_+$)

$$\psi(\vec{r}, sT_+) = \exp\left[-i\,H_0(sT_+ - sT_-) + izF_s\int_{sT_-}^{sT_+}\delta(t-sT)dt\right]\psi(\vec{r}, sT_-), \tag{22}$$

where $\psi(\vec{r}, sT_-)$ is the wave function before the kick ($t = sT_-$). Note that $sT_+ - sT_- \to 0$ and $\int_{sT_-}^{sT_+}\delta(t-sT)dt \equiv 1$.

Consequently, Eq. (22) is equivalent to the formula

$$\psi(\vec{r}, sT_+) = \exp(iF_s z)\psi(\vec{r}, sT_-). \tag{23}$$

In practical calculations we utilize the similar approximate procedure

$$\begin{aligned} \hat{\psi}_0 &= \psi(sT_-), \\ \left(I - \frac{\bar{\alpha}_\zeta^{(M)} F_s z}{2M}\right) \hat{\psi}_{\zeta/M} &= \left(I - \frac{\alpha_\zeta^{(M)} F_s z}{2M}\right) \hat{\psi}_{(\zeta-1)/M}, \qquad \zeta = 1, \ldots, M, \\ \psi(sT_+) &= \hat{\psi}_1, \end{aligned}$$

which conserves the unitarity and is correct up to the order $O(\|F_s z\|^{2M})$.

### 4.3. Galerkin representation

Performing the scaling transformations $\tilde{r} = r/n$, $\tilde{t} = t/n^2$, $\tilde{T} = T/n^2$ we present the solution as the Galerkin expansion

$$\psi(\vec{r}, t) = \sum_{l=0}^{l_{max}} \chi_l(\tilde{r}, \tilde{t}) Y_{lm}(\theta, \varphi), \tag{24}$$

where $Y_{lm}$ is a spherical function and the value of the truncation number $l_{max}$ depends on the parameters of the external field. In what follows, we restrict ourselves to the initial states with $m = 0$.

Using Eq. (24), we obtain from Eq. (1) with the Hamiltonian (16) a set of equations for the radial wave functions $\chi^T(\tilde{r}, \tilde{t}) = \{\chi_0(\tilde{r}, \tilde{t}), \chi_1(\tilde{r}, \tilde{t}), \ldots, \chi_{l_{max}}(\tilde{r}, \tilde{t})\}$:

$$i \frac{\partial \chi(\tilde{r}, \tilde{t})}{\partial \tilde{t}} = \left\{ H^{(0)}(\tilde{r}) + \left[\sum_{s=1}^{S} \delta(\tilde{t} - s\tilde{T})\right] H^{(1)}(\tilde{r}) \right\} \chi(\tilde{r}, \tilde{t}), \quad \chi(\tilde{r}, 0) = \chi^{(0)}(\tilde{r}) \tag{25}$$

with the boundary conditions

$$\lim_{\tilde{r} \to 0} \tilde{r}^2 \frac{\partial}{\partial \tilde{r}} \chi(\tilde{r}, \tilde{t}) = 0, \qquad \chi(\tilde{r}_{max}, \tilde{t}) = 0, \tag{26}$$

and normalization conditions in the interval $0 \le \tilde{r} \le \tilde{r}_{max}$

$$\int_0^{\tilde{r}_{max}} \tilde{r}^2 \tilde{\chi}^T(\tilde{r}, \tilde{t}) \chi(\tilde{r}, \tilde{t}) d\tilde{r} = 1 \tag{27}$$

The matrix elements of the $(l_{max} + 1) \times (l_{max} + 1)$ matrices $H^{(0)}$ and $H^{(1)}$ are given by

$$\begin{aligned} H^{(0)}_{ll'}(\tilde{r}) &= \left[-\frac{1}{2}\frac{1}{\tilde{r}^2}\frac{\partial}{\partial \tilde{r}}\tilde{r}^2\frac{\partial}{\partial \tilde{r}} + \frac{l(l+1)}{2\tilde{r}^2} - \frac{n}{\tilde{r}}\right]\delta_{ll'} + \beta^2 \frac{n^4 \tilde{r}^2}{8}\left\{\beta_z + (1-\beta_z)\left[1 - \frac{(l+1)^2}{4(l+1)^2 - 1} - \frac{l^2}{4l^2-1}\right]\right\}\delta_{ll'} \\ &\quad -\beta^2 \frac{n^4 \tilde{r}^2 (1-\beta_z)}{32\sqrt{(2l+1)(2l'+1)}} \frac{(l+l'+1)^2 - 1}{(l+l'+1)} \delta_{2,|l'-l|}, \end{aligned} \tag{28}$$

$$H^{(1)}_{ll'}(\tilde{r}) = -n\tilde{r}F_s \frac{\sqrt{(2l+1)(2l'+1)}}{2} \frac{l+l'+1}{(l+l'+1)^2 - 1} \delta_{1,|l-l'|}, \tag{29}$$

If $\beta = 0$, then the initial state $\chi(\tilde{r}, 0) = \chi^{(0)}$ takes the form

$$\chi_l^n(\tilde{r}, 0) = N_l R_{nl}(\tilde{r}), \quad \text{where} \quad R_{nl}(\tilde{r}) = \frac{2(2\tilde{r})^l \exp(-\tilde{r})}{\sqrt{n}(2l+1)!} \sqrt{\frac{(n+l)!}{(n-l-1)!}} {}_1F_1\left(-n+l+1, 2l+2, 2\tilde{r}\right), \tag{30}$$

$N_l$ is the normalization constant (calculated using (27) with the prescribed accuracy), and ${}_1F_1$ is the confluent hypergeometric function. For $\beta \neq 0$ we can find $\chi^{(0)} = \chi^{n\nu}$ from the eigenvalue problem for $H_0$ by means of the FEM code. For weak fields ($\beta \ll 1$) we can also use the perturbation theory implemented in terms of the irreducible representation of $so(4,2)$ algebra.[22, 26, 35]

### 4.4. Kantorovich representation

In the general case $\beta \neq 0$ we can present the solution as the Kantorovich expansion

$$\psi(\vec{r},t) = \sum_{i=1}^{n_{max}} \chi_i(\tilde{r},\tilde{t})\Phi_i(\theta,\varphi;\tilde{r}). \tag{31}$$

Here $\Phi_l(\theta,\varphi;\tilde{r})$ are eigenfunctions of the parametric eigenvalue problem

$$h_m(\tilde{r})\Phi_i(\theta,\varphi;\tilde{r}) = \frac{E_i(\tilde{r})}{2}\Phi_i(\theta,\varphi;\tilde{r}), \qquad \int \bar{\Phi}_i(\theta,\varphi;\tilde{r})\Phi_j(\theta,\varphi;\tilde{r})\sin\theta d\theta d\varphi = \delta_{ij},$$

$$h_m(\tilde{r}) = -\frac{1}{2}\left(\frac{1}{\sin\theta}\frac{\partial}{\partial\theta}\sin\theta\frac{\partial}{\partial\theta} - \frac{m^2}{\sin^2\theta}\right) + V_z(\tilde{r}), \qquad V_z(\tilde{r}) = \frac{m\beta}{2}\tilde{r}^2 + \frac{n^8}{8}\beta^2\tilde{r}^4[\beta_z + (1-\beta_z)\sin^2\theta]$$

with eigenvalues $E_i(\tilde{r})$ at any fixed $\tilde{r}$. The matrix elements of $(n_{max}) \times (n_{max})$ matrices $H^{(0)}$ and $H^{(1)}$ are given by

$$\begin{aligned} H^{(0)}_{ij}(\tilde{r}) &= -\frac{1}{2}\frac{I_{ij}}{\tilde{r}^2}\frac{\partial}{\partial\tilde{r}}\tilde{r}^2\frac{\partial}{\partial\tilde{r}} + \frac{U_{ij}(\tilde{r})}{\tilde{r}^2}\chi + \frac{1}{2}Q_{ij}(\tilde{r})\frac{d\chi}{d\tilde{r}} + \frac{1}{2}\frac{1}{\tilde{r}^2}\frac{d[\tilde{r}^2Q_{ij}(\tilde{r})\chi]}{d\tilde{r}} \\ H^{(1)}_{ij}(\tilde{r}) &= \int_0^\pi \sin\theta d\theta\bar{\Phi}_i(\theta,\varphi;\tilde{r})(-n\tilde{r}F_s\cos\theta)\Phi_j(\theta,\varphi;\tilde{r}) \end{aligned}$$

$U(r)$ and $Q(r)$ are finite $n_{max} \times n_{max}$ matrices whose elements are given by the relations

$$\begin{aligned} U_{ij}(\tilde{r}) &= \frac{E_i(\tilde{r}) + E_j(\tilde{r})}{4}\delta_{ij} - \frac{n}{\tilde{r}} + \frac{\tilde{r}^2}{2}H_{ij}(\tilde{r}), \quad H_{ij}(\tilde{r}) = H_{ji}(\tilde{r}) = 2\pi\int_0^\pi \sin\theta\frac{\partial\Phi_i}{\partial r}\frac{\partial\Phi_j}{\partial\tilde{r}}d\theta, \\ Q_{ij}(\tilde{r}) &= -Q_{ji}(\tilde{r}) = -2\pi\int_0^\pi \sin\theta\Phi_i\frac{\partial\Phi_j}{\partial\tilde{r}}d\theta, \quad I_{ij} = \delta_{ij}, \quad i,j = 1,2,\ldots,n_{max}. \end{aligned} \tag{32}$$

The value of the truncation number $n_{max}$ depends on the parameters of the external field $(\beta,\beta_z)$.

### 4.5. Scheme with total splitting of evolution operator

Thus, for evaluating the atomic evolution on a time grid

$$\Omega_{\tilde{\tau}} = \{\tilde{t}_0 = 0,\ \tilde{t}_{k+1} = \tilde{t}_k + \tilde{\tau},\ \tilde{t}_{max} = S\tilde{T},\ \tilde{\tau} = \tilde{T}/K\}$$

$(k = 0,\ldots,SK-1)$ the following computational algorithm is derived

$$\begin{aligned} \hat{\chi}^{(0)} &= \chi(\tilde{r},\tilde{t}_0), \\ \left[I + \frac{\bar{\alpha}^{(M)}_\zeta H^{(0)}(\tilde{r})\tilde{\tau}}{2M}\right]\hat{\chi}_{k+\zeta/M} &= \left[I + \frac{\alpha^{(M)}_\zeta H^{(0)}(\tilde{r})\tilde{\tau}}{2M}\right]\hat{\chi}_{k+(\zeta-1)/M}, \qquad k+\zeta/M \neq sK, \\ \left[I + \frac{\bar{\alpha}^{(M)}_\zeta H^{(0)}(\tilde{r})\tilde{\tau}}{2M}\right]\hat{\chi}_{sK;0} &= \left[I + \frac{\alpha^{(M)}_\zeta H^{(0)}(\tilde{r})\tilde{\tau}}{2M}\right]\hat{\chi}_{k+(\zeta-1)/M}, \qquad k+\zeta/M = sK, \\ \left[I + \frac{\bar{\alpha}^{(M)}_\zeta H^{(1)}(\tilde{r})}{2M}\right]\hat{\chi}_{sK;\zeta/M} &= \left[I + \frac{\alpha^{(M)}_\zeta H^{(1)}(\tilde{r})}{2M}\right]\hat{\chi}_{sK;(\zeta-1)/M}, \\ \hat{\chi}_{sK} &= \hat{\chi}_{sK;1}, \\ \chi(\tilde{r},S\tilde{T}) &= \hat{\chi}_{SK} \qquad (k = 0,\ldots,SK-1, s = 1,\ldots,S,\ \zeta = 1,\ldots,M). \end{aligned}$$

In case of $M = 1$ this scheme is reduced to the conventional splitting Crank-Nicholson algorithm for the kicked atom.

**Table 2.** The values of $\alpha(\tilde{t})$ and $Er(\tilde{t},j)$ calculated within the second-order ($\tilde{\tau}=\tilde{T}/64$), fourth-order ($\tilde{\tau}=\tilde{T}/16$), and sixth-order ($\tilde{\tau}=\tilde{T}/8$) schemes for a train of identical six kicks with $T=1028$ and $F=2\times10^{-3}$. Here $n=5$, $l_{max}$=6 and $\tilde{r}_{max}$=80.

| $s$ | order | $Er(\tilde{t},1)$ | $Er(\tilde{t},2)$ | $Er(\tilde{t},3)$ | $\alpha(\tilde{t})$ | $s$ | order | $Er(\tilde{t},1)$ | $Er(\tilde{t},2)$ | $Er(\tilde{t},3)$ | $\alpha(\tilde{t})$ |
|---|---|---|---|---|---|---|---|---|---|---|---|
| 1 | 2nd | 0.17123 | 0.04128 | 0.00828 | 1.97713 | 4 | 2nd | 0.67243 | 0.16510 | 0.03320 | 1.94354 |
| | 4th | 0.07030 | 0.00473 | 0.00028 | 3.88197 | | 4th | 0.28125 | 0.01921 | 0.00199 | 3.92720 |
| | 6th | 0.04495 | 0.00861 | 0.00014 | 5.70142 | | 6th | 0.18148 | 0.00464 | 0.00095 | 5.58270 |
| 2 | 2nd | 0.34128 | 0.08258 | 0.01658 | 1.97072 | 5 | 2nd | 0.83054 | 0.20612 | 0.04146 | 1.92303 |
| | 4th | 0.14070 | 0.00954 | 0.00097 | 3.93554 | | 4th | 0.35029 | 0.02395 | 0.00183 | 3.88293 |
| | 6th | 0.09031 | 0.00202 | 0.00087 | 6.26054 | | 6th | 0.22551 | 0.00550 | 0.00100 | 5.60993 |
| 3 | 2nd | 0.50887 | 0.12389 | 0.02491 | 1.95963 | 6 | 2nd | 0.98214 | 0.24689 | 0.04971 | 1.89869 |
| | 4th | 0.21122 | 0.01441 | 0.00176 | 3.96044 | | 4th | 0.41848 | 0.02862 | 0.00198 | 3.87135 |
| | 6th | 0.13620 | 0.00343 | 0.00132 | 5.97308 | | 6th | 0.26911 | 0.00628 | 0.00103 | 5.64531 |

## 5. NUMERICAL RESULTS

In this Section we present the numerical results obtained using the computational method developed above. The spatial part of the problem is treated by means of the FEM.

Let us introduce the time-dependent discrepancy functions

$$Er^2(\tilde{t},j)=\sum_{l=0}^{l_{max}}\int_0^{\tilde{r}_{max}}\left|\chi_l(\tilde{r},\tilde{t})-\chi_l^{\tilde{\tau}_j}(\tilde{r},\tilde{t})\right|^2\tilde{r}^2d\tilde{r}, \tag{33}$$

where $\chi_l^{\tilde{\tau}_j}(\tilde{r},\tilde{t})$ is the numerical solution for the time step $\tilde{\tau}_j=\tilde{\tau}/2^{j-1}$, $j=1,2,3$. The function $\chi_l(\tilde{r},\tilde{t})$ corresponds to the time step $\tilde{\tau}/8$. Using the values $Er(\tilde{t},j)$, we calculate the convergence rate $\alpha(\tilde{t})$ of the calculation scheme (33) as follows

$$\alpha(\tilde{t})=\log_2\left|\frac{Er(\tilde{t},1)-Er(\tilde{t},2)}{Er(\tilde{t},2)-Er(\tilde{t},3)}\right|. \tag{34}$$

The functions $Er(\tilde{t},j)$ and $\alpha(\tilde{t})$ have been examined in the case of a train of six identical kicks with $T=1028$ and $F=2\times10^{-3}$. In order to determine the solution $\chi_l^n(\tilde{r},\tilde{t})$ in space, we employed the finite element grid $\Omega_{\tilde{r}}=\{\tilde{r}_{min}=0,(50),10,(100),\tilde{r}_{max}=80\}$, where the numbers in round brackets stand for the numbers of nodes in the corresponding intervals. Between each two nodes the Lagrange interpolation polynomials of the sixth order have been applied. Table 2 presents the values of $Er(\tilde{t},j)$ (see Eq. (33)) and $\alpha(\tilde{t})$ (see Eq (34)) obtained using the second-order scheme (that amounts to the Crank-Nicholson scheme) and the implicit fourth- and sixth-order schemes in the case $n=5$ and $l_{max}=6$. Here $\tilde{\tau}=\tilde{T}/64$ for the Crank-Nicholson scheme and $\tilde{\tau}=\tilde{T}/16$ and $\tilde{T}/8$ for the implicit fourth-order and sixth-order schemes, respectively. As it can be clearly seen, although the implicit schemes involve the larger time steps $\tilde{\tau}$ than the Crank-Nicholson scheme does, however they provide a substantially better accuracy and the convergence rate in the interval $[t_0,6\tilde{T}]$ where $\tilde{T}=T/n^2=T/25$. However, to have similar estimations on a more large time interval $[t_0,t_{max}]$ one needs to use nonuniform grid $\Omega_\tau$, to choose the smaller time step $\tilde{\tau}$ at least in the vicinity of the kick time moment, in accordance with theoretical estimations (6), and to use high-precision calculation similar to shown in Fig. 4, or to use diffused $\delta$-functions with the Gaussian-like form-factor.[27]

Employing the sixth-order implicit scheme, we performed the calculations for the same situation as in Ref.,[30] where the evolution of initial parabolic state $|n_1=4,n_2=4,m=0\rangle$ in a train of kicks with the period $T=5357$ and the strength $F=2\times10^{-3}$ was investigated. The numerical results for the probabilities $P_{n=9}=\sum_{l=0}^{8}|\langle9,l,0|\psi(t)\rangle|^2$ and $P_{n=10}=\sum_{l=0}^{9}|\langle10,l,0|\psi(t)\rangle|^2$ are shown in Fig. 5a. They markedly agree with those of Ref..[30] In accordance with $T_n=2\pi/[1/2n^2-1/2(n+1)^2]$ the period $T=5357$ corresponds to a resonance regime between the two states with $n=9$ and $n=10$, respectively. However, as noted in Ref.,[30] the observed picture is more complicated than a two-state resonance due to the damping arising from ionization and Rabi-like oscillations. Recall that the value of magnetic quantum number ($m=0$) is conserved.

**Table 3.** The first- and second-order perturbation theory corrections $E_{pt}^{(1)}$ and $E_{pt}^{(2)}$, respectively, for a hydrogen atom in a magnetic field with strength $\beta = 1.472 \times 10^{-5}$ in the cases $\beta_z = 0$ and $\beta_z = 2$. The FEM corrections $\delta E_{gal} = E_{gal} - E^{(0)}$ and $\delta E_{kant} = E_{kant} - E^{(0)}$ to the unperturbed value $E^{(0)} = -1/2n^2$ for $n = 9$ ($E^{(0)} = -6.1728395 \times 10^{-3}$) calculated by Galerkin and Kantorovich methods are also shown. All energy values are scaled to $10^7$.

| | $\beta_z = 0$ | | | | $\beta_z = 2$ | | | |
|---|---|---|---|---|---|---|---|---|
| $\nu$ | $E_{pt}^{(1)}$ | $E_{pt}^{(1)} + E_{pt}^{(2)}$ | $\delta E_{gal}$ | $\delta E_{kant}$ | $E_{pt}^{(1)}$ | $E_{pt}^{(1)} + E_{pt}^{(2)}$ | $\delta E_{gal}$ | $\delta E_{kant}$ |
| 0 | 0.414 1701 | 0.414 1576 | 0.414 1579 | 0.414 1840 | 3.05 385 | 3.05 369 | 3.05 369 | 3.05 371 |
| 1 | 0.418 4732 | 0.418 4596 | 0.418 4599 | 0.418 4862 | 3.69 134 | 3.69 112 | 3.69 112 | 3.69 115 |
| 2 | 0.916 5774 | 0.916 5585 | 0.916 5586 | 0.916 5684 | 4.17 005 | 4.16 979 | 4.16 979 | 4.16 979 |
| 3 | 1.105 188 | 1.105 147 | 1.105 147 | 1.105 162 | 4.74 866 | 4.74 831 | 4.74 831 | 4.74 832 |
| 4 | 1.499 518 | 1.499 452 | 1.499 452 | 1.499 470 | 4.81 374 | 4.81 340 | 4.81 340 | 4.81 340 |
| 5 | 1.981 345 | 1.981 247 | 1.981 247 | 1.981 264 | 6.02 268 | 6.02 214 | 6.02 214 | 6.02 214 |
| 6 | 2.566 782 | 2.566 648 | 2.566 649 | 2.566 671 | 6.02 298 | 6.02 244 | 6.02 244 | 6.02 244 |
| 7 | 3.252 108 | 3.251 935 | 3.251 936 | 3.251 968 | 7.82 700 | 7.82 621 | 7.82 621 | 7.82 621 |
| 8 | 4.036 587 | 4.036 373 | 4.036 373 | 4.036 436 | 7.82 700 | 7.82 621 | 7.82 621 | 7.82 621 |

Let us turn to the situation when the hydrogen atom is kicked in the presence of magnetic field parallel to the $z$ axis. We take the magnetic field strength $\beta = 1.472 \times 10^{-5}$ which is typical for the magnetic traps.[31,32] Note that such a field strength is also of interest for the studies of recombination processes involving the excited states with $n = 8, 9, \ldots, 19$ and the metastable state with $n = 2$ of an antihydrogen atom, where the Lamb shift can be observed and thus the CPT invariance can be tested.[33] Table 3 shows the results of the present FEM calculations for energy eigenvalues of the multiplet $|n = 9, \nu = 0 \ldots n-1, m\rangle$. The case $\beta_z = 0$ amounts to the well-known quadratic Zeeman effect, while the case $\beta_z = 2$ resembles the van der Waals interaction between an atom and a metallic surface (see, e.g., the paper[34] and references therein). The energy corrections calculated using FEM coincide with those of the first-order perturbation calculations up to the fourth digit.

We inspected the possibility of realizing the two-state resonance regime for the Zeeman states. Fig. 5b shows the numerical results for the probabilities $P_{n=9}$ and $P_{n=10}$ in the case $\beta_z = 0$ for the initial Zeeman state $|n = 9, \nu = 0, m\rangle$ that, according to Table 3, has the minimal energy within the $n = 9$ manifold. In contrast to the results presented in Fig. 5a, a marked signature of two-state resonance regime is observed. A slight decay of the total probability $P_{n=9} + P_{n=10}$ is also observed. The role of the initial Zeeman state in the realization of the two-state resonance regime can be seen from Fig. 5c, namely, the picture obtained for the initial state $|n = 9, \nu = 8, m = 0\rangle$, which has the maximal energy within the $n = 9$ manifold in the case $\beta_z = 0$, is more complicated than the two-state resonance picture obtained for $|n = 9, \nu = 0, m = 0\rangle$. Finally, the role of the external field configuration (17) is reflected in Fig. 5d, where the probabilities $P_{n=9}$ and $P_{n=10}$ for the initial state $|n = 9, \nu = 0, m\rangle$ in the case $\beta_z = 2$ are presented. The results resembling those in Fig. 5a exhibit no clear signature of the two-state resonance regime.

## 6. CONCLUSION

A new computational approach is proposed for the solution of the time-dependent Schrödinger equation (TDSE), in which the numerical scheme based on the finite-element method (FEM) is efficiently incorporated. Multi-layer operator-difference schemes for TDSE with the effective Hamiltonians are constructed from the original time-dependent Hamiltonian by means of the Magnus expansion and the Pade-approximation. In order to solve the TDSE with the effective Hamiltonian thus obtained, the FEM is applied for the discretization of the spatial domain which brings the operator-difference scheme to the algebraic form. The additional gauge transformation of the operator-difference schemes is applied to improve the finite-element discretization. The efficiency and accuracy of the numerical scheme associated with Galerkin and Kantorovich reduction with respect to the angular variables and FEM with respect to the radial variable is confirmed in the second-, fourth-, and sixth-order time-step computations for several integrable atomic models with external fields. Our approach would be

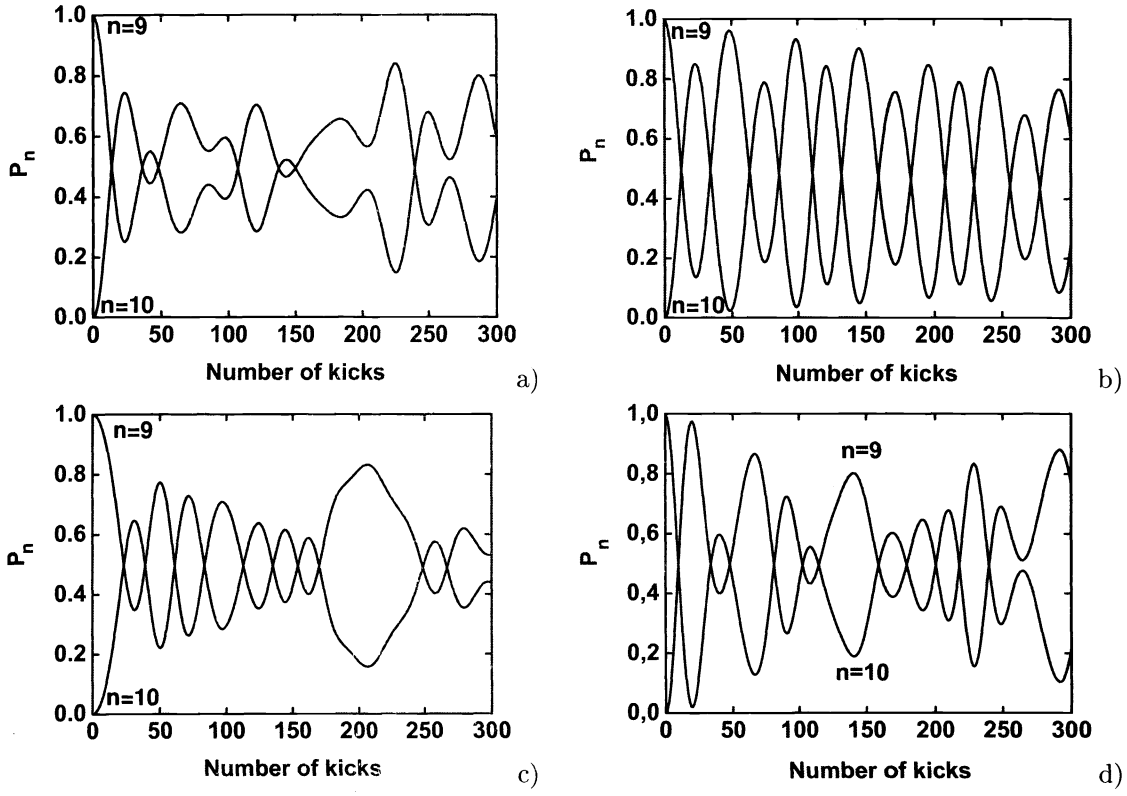


**Figure 5.** The occupation probabilities $P_{n=9}$ and $P_{n=10}$ for the initial: a) parabolic state $|n=9, n_1=n_2=4, m=0\rangle$, b) Zeeman state $|n=9, \nu=0, m=0\rangle$ at $\beta_z=0$, c) Zeeman state $|n=9, \nu=8, m=0\rangle$ at $\beta_z=0$, d) Zeeman state $|n=9, \nu=0, m=0\rangle$ at $\beta_z=2$.

worth being applied to the quantum control problem, some pre-experimental calculations in the atomic dynamics in traps and/or external pulse fields.

## 7. ACKNOWLEDGMENTS

This work was partly supported by Grants of RFBR Nos. 06-01-00385-a, 06-02-16885-a, 06-02-17003-a, 06-02-91167-a, and Grant of the President of the Bulgarian State Agency for Atomic Energy (2004), by Grant I-1402/2004 of the Bulgarian Fund for Scientific Investigations.

## REFERENCES

1. F.H.M. Faisal, Y.I. Salamin, Electron dynamics and photon-emission spectra in an ultrashort laser pulse and a uniform magnetic field, Phys. Rev. A, **60**, 2505 (1999).
2. Y.I. Salamin and F.H.M. Faisal, Ultrahigh electron acceleration and Compton emission spectra in a super-intense laser pulse and a uniform axial magnetic field, Phys. Rev. A **61**, 043801 (2000);
3. P. Krekora, R.E. Wagner, Q. Su, and R. Grobe, Dirac theory of ring-shaped electron distributions in atoms, Phys. Rev. A **63**, 025404 (2001).
4. A.D. Bandrauk and H.Z. Lu, Enhanced ionization of the molecular ion $H_2^+$ in intense laser and static magnetic fields, Phys. Rev. A **62**, 053406 (2000).
5. V.M. Rylyuk and J. Ortner, Decay of a weakly bound level in a monochromatic electromagnetic field and a static magnetic field, Phys. Rev. A **67**, 013414 (2003).
6. P. Schlagheck, D. Pingel, and P. Schmelcher, Collinear helium under periodic driving: Stabilization of the asymmetric stretch orbit, Phys. Rev. A **68**, 053410 (2003).

7. M. Gavrila, Atomic stabilization in superintense laser fields, J. Phys. B: At. Mol. Opt. Phys. **35**, R147 (2002).
8. A.M. Popov, O.V. Tikhonova, and E.A. Volkova, Strong-field atomic stabilization: numerical simulation and analytical modelling, J. Phys. B: At. Mol. Opt. Phys. **36**, R125 (2003).
9. V.L. Derbov, L.A. Melnikov, I.M. Umansky, and S.I. Vinitsky, Multipulse laser spectroscopy of p-bartHe+: Measurement and controlof the metastable state populations, Phys. Rev. A **55**, 3394 (1997).
10. I.M. Umansky, L.A. Melnikov, V.L. Derbov, M.V. Ryabinina, and S.I. Vinitsky, Free-bound transitions in the process of positron-antiproton collisions in external laser pulse, field Phys. Atomic Nuclei **61**, 1928 (1998).
11. M. V. Ryabinina, L. A. Melnikov, "Phase-Sensitive Ionization and Recombination of Anti-Hydrogen Atom Using Zero-Duration High Intensity Laser Pulse", AIP Conference Proceedings **796**, pp.325-329, 2005.
12. E.Y. Sidky and B.D. Esry, Boundary-Free Propagation with the Time-Dependent Schrodinger Equation, Phys. Rev. Lett. **85**, 5086 (2000).
13. Yu.V. Popov, K.A. Kouzakov, A.A. Gusev, and S.I. Vinitsky, Model of interaction of zero-duration laser pulses with an Atom. Proc. SPIE **5067**, 199 (2003).
14. G.I. Marchuk, in *Partial Differential Equations. II SYNSPADE-1970* (Academic Press, New-York, London, 1971).
15. V.L. Derbov, M.S. Kaschiev, V.V. Serov, A.A. Gusev, and S.I. Vinitsky, Adaptive numerical methods for time-dependent Schroedinger equation in atomic and laser physics, Proc. SPIE **5069**, 52 (2003).
16. G. Strang and G. Fix, *An Analisys of The Finite Element Method* (Englewood Cliffs, Prentice Hall, New York, 1973).
17. K.J. Bathe, *Finite Element Procedures in Engineering Analysis* (Englewood Cliffs, Prentice Hall, New York, 1982).
18. S.I. Vinitsky, V.P. Gerdt, A.A. Gusev, M.S. Kaschiev, V.A. Rostovtsev, V.N. Samoylov, T.V. Tupikova, Y. Uwano, Symbolic Algorithm for Factorization of the Evolution Operator of the Time-Dependend Schrodinger Equation Programming and Computer Software, (2006); Programmirovanie, (2006).
19. A. Gusev, V. Gerdt, M. Kaschiev, V. Rostovtsev, V. Samoylov, T. Tupikova, Y. Uwano, and S. Vinitsky, Symbolic-Numerical Algorithm for Solving the Time-Dependent Schrodinger Equation by Split-Operator Method, Computer Algebra in Scientific Computing 8th International Workshop, CASC 2005, Kalamata, Greece, September 12-16, 2005, Proceedings Series: Lecture Notes in Computer Science **3718**, 244-258 (2005).
20. I.V. Puzynin, A.V. Selin, and S.I. Vinitsky, A high-order accuracy method for numerical solving of the Time-Dependent Schroedinger equation, Comput. Phys. Commun. **123**, 1 (1999); Magnus-factorized method for numerical solving of the time-dependent Schroedinger equation, Comput. Phys. Commun. **126**, 158 (2000).
21. N.G. Bankov, M.S. Kaschiev, and S.I. Vinitsky, Adaptive method for solving the time-dependent Schrödinger equation Comptes rendus de l'Akademie bulgare des Scienses **55**, 25 (2002).
22. A.A. Gusev, O. Chuluunbaatar, M.S. Kaschiev and S.I. Vinitsky, High accuracy splitting algorithms for the time-dependent Schrodinger equation with a train of laser pulses, Proc. SPIE **5476**, 100 (2004).
23. A.G. Abrashkevich, D.G. Abrashkevich, M.S. Kaschiev, and I.V. Puzynin, Finite-element solution of the coupled-channel Schrodinger equation using high-order accuracy approximations, Comput. Phys. Commun. **85**, 40 (1995).
24. A.G. Abrashkevich, M.S. Kaschiev, and S.I. Vinitsky, A New Method for Soling an Eigenvalue Problem for a System Of Three Coulomb Particles within the Hyperspherical Adiabatic Representation, J. Comput. Phys. **163**, 328 (2000).
25. M. G. Dimova, M. S. Kaschiev, S. I. Vinitsky, "The Kantorovich method for high-accuracy calculations of a hydrogen atom in a strong magnetic field: low-lying excited states", *Journal of Physics B: Atomic, Molecular and Optical Physics* **38**, pp. 2337-2352, 2005.
26. A.A. Gusev, V.N. Samoilov, V.A. Rostovtsev, S.I. Vinitsky, Algebraic perturbation theory for Hydrogen atom in a weak electric fields, Programmirovanie, 27-31, (2001); Programming and Computer Software 18-21, (2001).

27. Yu.V. Popov, V.V. Sokolovsky, A.A. Gusev, S.I. Vinitsky, Separable potentials like a bridge between continuous and discrete scattering theories, Proc. SPIE **5476**, 75 (2004).
28. V.L.Derbov, M.S.Kaschiev, V.V.Serov, A.A.Gusev, S.I.Vinitsky, Adaptive numerical methods for time-dependent Schroedinger equation in atomic and laser physics. Proc. SPIE **5069**, pp. 52-60, (2003).
29. A.M. Ermolaev, I.V. Puzynin, A.V. Selin, S.I. Vinitsky, Integral boundary condition for the time-dependent Schodinger Equation: Atom in a laser field, Phys. Rev. A, **60**, 1999, p.4831-4845.
30. A.K. Dhar, M.A. Nagarajan, F.M. Israilev, and R.R. Whitehead, Persistence of two-state resonances in a hydrogen atom under the influence of a periodic impulsive field, J. Phys. B: At. Mol. Phys. **16**, L17 (1983).
31. M.H. Holzscheiter and M. Charlton, Ultra-low energy antihydrogen, Rep. Prog. Phys. **62**, 1 (1999).
32. M. Amoretti *et al.*, Phys. Lett. B **590**, 133 (2004).
33. Th. Udem *et al.*, Phase-Coherent Measurement of the Hydrogen 1S-2S Transition Frequency with an Optical Frequency Interval Divider Chain, Phys. Rev. Lett. **79**, 2646 (1997).
34. V.S. Melezhik, Nonperturbative behavior of a hydrogen atom in a van der Waals field, Phys. Rev. A **52**, R3393 (1995).
35. M.J. Engenfield, *Group Theory and the Coulomb Problem* (Victoria, Monash university, 1972).